Agroecosystem-Driven Rhizoplane Bacteriome Assembly in Cassava Uncovers Bacillus-Mediated Suppression of Stem and Root Rot

Divya Santha
Indian Agricultural Research Institute
Tusar Kanti Bag
Indian Agricultural Research Institute
Makeshkumar Thangaraj
Central Tuber Crops Research Institute
Jeeva Muthulekshmi Lajapathi
Central Tuber Crops Research Institute
Binoy Ambika Manirajan
School of Biosciences,Mahatma Gandhi University
Vinod Chouhan
Indian Agricultural Research Institute
Veena Syamala Swayamvaran
Central Tuber Crops Research Institute
Kumar Aundy
kumar@iari.res.in

Indian Agricultural Research Institute

Research Article

Keywords: 16S rRNA metabarcoding, Bacillus subtilis, Biological control, Core Microbiome, Fusarium falciforme, Manihot esculenta

Posted Date: June 29th, 2026

DOI: https://doi.org/10.21203/rs.3.rs-10099516/v1

Additional Declarations: No competing interests reported.

Abstract

Cassava (*Manihot esculenta*Crantz) stem and root rot caused by *Fusarium falciforme* is a major constraint to production. This study characterised rhizoplane bacteriome shifts across agroecosystems with contrasting disease incidence and identified microbial indicators and potential biocontrol agents using 16S rRNA gene amplicon sequencing, culture-dependent isolation, and functional assays. Microbial richness was highest in diseased wetlands (Chao1: 601.60 ± 10.37), followed by healthy wetlands (581.20 ± 14.39) and uplands (547.97 ± 5.74), while evenness remained comparable among ecosystems. Pseudomonadota dominated all sites (~ 64%). Bacteroidota, Planctomycetota, and Actinomycetota were enriched in healthy wetlands but declined in diseased sites, whereas Verrucomicrobiota increased in diseased roots (7.35%). *Pseudomonas* dominated uplands (29.7%), while *Aeromonas, Salmonella, and Devosia* were associated with disease. The conserved core microbiome comprised *Aquicella, Enterobacter, Klebsiella, Sodalis*, and *Salmonella.* Network analysis identified Geminigeraceae as a keystone taxon and revealed predominantly cooperative interactions between bacteria and fungi. Among 195 isolates, *Bacillus subtilis* ULB_36 and *Bacillus stercoris* ULB_12 exhibited strong inhibition of *F. falciforme* (83.33% and 78.52%), significantly reduced disease severity, and enhanced plant growth, comparable to fungicide treatments. These findings demonstrate that cassava stem and root rot are associated with disruption of the rhizoplane bacteriome and the loss of beneficial taxa. Agroecosystem-specific microbial signatures and core bacteriome members provide insights into cassava–microbe interactions, while native *Bacillus* strains offer promising niche-adapted biocontrol solutions for sustainable management of cassava stem and root rot.

Introduction

The plant rhizoplane, the zone between the root epidermis and the surrounding soil, is a dynamic microbial habitat crucial for microbial colonisation and for shaping root microbiomes (Edwards et al. 2015). This zone is especially vital for root and tuber crops such as cassava, where microbial communities influence nutrient uptake, storage root development, stress tolerance, and pathogen protection. Cassava (*Manihot esculenta*Crantz) is a key source of dietary carbohydrates in the tropics, supporting over 800 million people and proving resilient to drought, poor soils, and erratic rainfall—traits that make it essential under climate change (Howeler et al. 2013; Mohidin et al. 2023; Immanuel et al. 2024). As climate variability increases, cassava's importance in marginal farming areas expands, yet diseases such as stem and root rot by *Fusarium*threaten its productivity (Silva et al. 2022). This pathogen infects underground tissues, often asymptomatically early on, and can cause severe losses, sometimes nearly 100% (Oliveira et al. 2013). The emergence of additional *Fusarium* species increases management challenges (da Silva et al. 2025), as infections occur below ground and symptoms appear late. Current control methods—fungicides and cultural practices—are often ineffective and unsustainable and can harm beneficial microbes, thereby reducing natural disease resistance (Busby et al. 2017; Vannier et al. 2019). There is a pressing need for alternative, eco-friendly strategies that leverage natural biological processes.

Recent plant microbiome research shows that plant health depends on the microbiome, particularly the rhizoplane bacteriome, which supports nutrient cycling, pathogen exclusion, stress adaptation, and the production of antimicrobial compounds (Toju et al. 2018; Vannier et al. 2019). Microbial interactions mediated by volatile compounds and secondary metabolites also help suppress pathogens and enhance plant resilience (Tyc et al. 2017). Microbiome-based strategies are emerging as sustainable approaches to enhance crop resilience and reduce reliance on chemicals under challenging conditions.

Network analyses show that highly connected "hub" microbes shape microbiome structure and stability by mediating interactions (Agler et al. 2016). The concept of a "core microbiome"—taxa consistently associated with the host across environments—suggests that plants selectively maintain beneficial microbes that are critical for stability and resilience (Toju et al. 2018). Understanding these communities is key to identifying microbial indicators of plant health and to developing microbiome-based disease management strategies.

Despite advances, the structure and dynamics of the cassava rhizoplane bacteriome across diverse environments, including disease-endemic wetlands and disease-suppressive uplands, remain poorly understood. Key knowledge gaps include how agroecosystems shape microbial assembly, how disease alters interactions, and which taxa contribute to natural suppression. Addressing these gaps is vital for understanding microbiome-driven resistance and for developing sustainable controls.

This study used high-resolution 16S rRNA metabarcoding, network analysis, culture-based validation, and bioassays to characterise the cassava rhizoplane bacteriome in healthy and diseased plants in Kerala, India. The goals were to identify core taxa in disease-suppressive environments, understand microbial networks, and test the antagonistic and growth-promoting potential of key bacteria. The results offer insights into the role of microbiome stability in suppressing cassava stem and root rotand lay the groundwork for microbiome-based, climate-smart disease management to ensure sustainable cassava cultivation.

Materials and Methods

Study Location and Sample Collection

We performed amplicon sequencing (metabarcoding) of the cassava rhizoplane bacteriome, targeting the V3–V4 region of the bacterial 16S rRNA gene (Klindworth et al. 2013). Samples were collected in December 2024 from two cassava-growing regions in Thiruvananthapuram, Kerala, India: Venganoor (8.408601°N, 76.989631°E, 44 m elevation), a wetland agroecosystem endemic for cassava stem and root rot, and Neyyattinkara (8.383752°N, 76.998306°E, 26 m elevation), a non-endemic upland agroecosystem. The study used a locally cultivated cassava variety susceptible to stem and root rot. Root samples from eight-month-old plants—healthy and diseased from the wetland, and healthy from the upland—were collected in triplicate, with each replicate combining 3–5 neighbouring plants. After removing loose soil, roots were aseptically placed in sterile Falcon tubes and transported in cooled containers (4.0 ± 1.0°C) for microbiome analysis.

Profiling of Rhizoplane Microbiome by Metabarcoding

Rhizoplane Microbial Community DNA Extraction

Root samples (10 g) were washed with sterile PBST (8.1 mM Na_2HPO_4, 1.5 mM KH_2PO_4, 137 mM NaCl, 2.7 mM KCl, pH 7.4, 0.1% Tween-20) until clear. The rhizoplane microbiome was extracted by agitating roots in 50 mL of sterile PBST at 250 rpm for 30 min at 28°C, vortexing for 10 s, and repeating the process 6 times to obtain 300 mL. Final washes were plated to confirm sterility. The suspension was centrifuged at 12,000 × g for 30 min at 4°C to pellet microbes for microbiome analysis, following Lundberg et al. (2012) and Zhang et al. (2021). Genomic DNA was extracted using the NucleoSpin® Soil Kit, and concentration and purity were assessed using a NanoDrop™ spectrophotometer and gel electrophoresis. The V3–V4 region of 16S rRNA was amplified using primers V3F (5'-CCTACGGGNGGCWGCAG-3') and V4R (5'-GACTACHVGGGTATCTAATCC-3')with Illumina overhangs in 50 µL reactions containing 100 ng DNA, 0.5 µM primers, and KAPA master mix. PCR was performed on a Veriti™ Pro Cycler with an initial denaturation at 98°C for 2 min, followed by 35 cycles of 98°C for 10 s, 58°C for 15 s, and 72°C for 40 s, and a final extension at 72°C for 7 min. Amplicons were confirmed by gel electrophoresis, quantified by NanoDrop™, purified with KAPA HyperPure Beads, and sequenced on the Illumina NextSeq platform.

Preparation of Sequencing Libraries

PCR products with Illumina adapters were amplified with i5 and i7 primers to add dual-index barcodes and flow-cell-binding sites (P5 and P7) as per the Illumina protocol. Libraries prepared using the Illumina DNA Prep kit were purified with KAPA HyperPure Beads (Roche) and quantified using a Qubit 4 Fluorometer and the dsDNA HS Assay Kit (Thermo Fisher). Size and integrity were assessed using an Agilent TapeStation 4150 with a D1000 ScreenTape. Libraries were pooled to equal molarity and sequenced on an Illumina NextSeq 2000 with paired-end 300-bp reads.

Bioinformatics Analysis and Taxonomic Classification

Raw sequencing reads were assessed for quality using FastQC (v0.11.9; Wingett and Andrews 2018), which analysed base quality, GC content, length distribution, duplication, overrepresented sequences, adapter contamination, and k-mer content. Low-quality bases and residual adapters were trimmed with fastp (v0.23.2; Chen et al. 2018) using a Q20 cutoff and a minimum length of 20 bp. Reads with > 10% ambiguous bases, > 50% bases below Q30, or shorter than 30 bp were removed. Taxonomic classification was performed using Kraken2 (v2.1.2; Wood et al. 2019) against the RefSeq-based database (as on 12 January 2024) and refined with Bracken (v2.7; Lu et al. 2017) to obtain accurate species-level abundance estimates, enabling robust microbial profiling.

Community Composition and Diversity Analyses

Microbial community structure and taxonomic profiles were visualised using R tools, including bar plots with ggplot2 (v3.4.0; Wickham 2016). Diversity was measured using phyloseq (v1.42.0; McMurdie and Holmes 2013), vegan (v2.6-4; Oksanen et al. 2026), and within MicrobiomeAnalyst 2.0 (Dhariwal et al. 2017). Alpha diversity metrics, such as ACE, Chao1, Shannon, and Simpson indices, were used to assess richness and evenness. Beta diversity was assessed using NMDS based on Bray–Curtis dissimilarities, with significance tested by PERMANOVA (999 permutations). Rarefaction curves were used to evaluate sequencing depth and species richness.

Core Microbiome and Shared OTU Analysis

For core microbiome identification, a prevalence cutoff of 20% and a relative abundance threshold of 0.01% were applied using MicrobiomeAnalyst 2.0. Upset plots were generated in R (version 2022.12.0) using UpsetR to examine OTU distributions and overlaps across sample groups. OTU presence–absence data were imported with readxl and processed with dplyr and tidyr. This enabled visualisation of shared and unique OTUs across soil environments, thereby advancing understanding of microbial community structure and diversity.

Hub Taxa and Co-occurrence Network Analysis

Co-occurrence network analysis identified hub taxa from species abundance profiles derived from Kraken2 outputs. Bacterial and fungal (mycobiome) data from previous studies were combined to examine inter-kingdom interactions. Pairwise Spearman correlations ($|r| \geq 0.5$, $p < 0.05$) were computed using SciPy with FDR correction. The network, built with NetworkX, used nodes to represent taxa and edges to represent significant positive (red) or negative (blue) correlations. Centrality metrics (degree, betweenness, closeness) identified keystone taxa, and significance was assessed via 1,000 permutations. Visualisations were produced using Matplotlib and Seaborn, and bar plots of hub taxa abundances were generated using pandas.

Culture-Dependent Analysis and Validation of Metabarcoding-Based Taxa

Isolation of the Culturable Rhizoplane Microbiome

The same samples used for metabarcoding were also cultured to isolate bacteria and validate OTUs from V3-V4 sequencing. The microbial concentrate was serially diluted up to 10^{-7}, and 1 mL aliquots at 10^{-4} to 10^{-7} were spread on Nutrient Agar (peptone 5.0 g; beef extract 3.0 g; NaCl 5.0 g; agar 15.0 g; pH 7.0 ± 0.2) and Minimal media (Na2HPO4 33.9 g; NaCl 2.5 g; KH2PO4 15.0 g; NH4Cl 5.0 g; pH 7.0 ± 0.2)to recover diverse bacteria. Each treatment had three

biological and three technical replicates. Plates were incubated at 28 ± 2°C for 2–3 days, and isolates were purified by streaking and identified morphologically. Cultures were stored in 30% glycerol at -20°C and − 80°C for long-term storage.

Bacterial Identification by 16S rRNA Gene Sequencing

Genomic DNA was extracted from fresh bacterial cultures using a modified CTAB method (Moore et al. 2008). Its quality and quantity were assessed by agarose gel electrophoresis and NanoDrop spectrophotometry, and samples were normalised to 100 ng/µL for downstream analysis. Genetic diversity was evaluated using BOX-PCR fingerprinting (Versalovic et al. 1998); identical patterns indicated duplicates, which were excluded. Non-duplicate isolates were preserved. PCR amplified the full-length 16S rRNA gene with primers 27F (5'-AGAGTTTGATCCTGGCTCAG-3') and 1492R (5'-GGTTACCTTGTTACGACTT-3'): initial denaturation at 98°C for 2 min, followed by 35 cycles of 98°C for 10 s, 58°C for 15 s, 72°C for 40 s, and a final extension at 72°C for 7 min. PCR products were verified on agarose gels, purified, and bidirectionally sequenced. Sequences were assembled, edited, compared with NCBI GenBank and SILVA for taxonomic identification, and deposited in GenBank. OTU cross-referencing validated taxonomy, and isolates were assessed for inclusion in the core microbiome.

Screening and Greenhouse Evaluation of Antagonistic Rhizoplane Bacterial Isolates against Fusarium falciforme

The antagonistic potential of 195 rhizoplane bacterial isolates against *Fusarium falciforme* (CTCRI 03 FP; GenBank PV982217.1) was assessed using dual-culture and volatile-inhibition assays, followed by greenhouse validation of selected isolates. In the dual culture assay, a 5-mm mycelial disc of the pathogen was placed at the centre of a PDA plate, with bacterial isolates streaked at equal intervals around the disc, and fungal growth inhibition was recorded after incubation at 25–28°C for 7 days. In the volatile inhibition assay, bacterial isolates grown on nutrient agar for 48 h were inoculated (10 µL; ~10^8 CFU mL^{-1}; OD_{600} ≈ 1.0) onto nutrient agar plates, while fungal discs were placed on PDA plates; both plates were sealed face-to-face with Parafilm to assess inhibition mediated by bacterial volatile organic compounds. Both assays were conducted with three replicates and repeated three times. Percentage inhibition was calculated using Vincent's formula: PI (%) = ((Rc − Rt)/Rc) × 100, where Rc and Rt represent radial growth in control and treatment plates, respectively (Vincent, 1947). The average inhibition values from both assays were used to rank isolates and select promising candidates for greenhouse evaluation. The biocontrol efficacy of *Bacillus subtilis* ULB_36 and *Bacillus stercoris* ULB_12 was subsequently evaluated against *F. falciforme* in a greenhouse experiment using a susceptible local cassava variety. The pathogen inoculum was prepared on a sand–maize meal medium containing washed river sand (900 g), maize meal (100 g), and distilled water (200 mL), followed by incubation at 28 ± 2°C for two weeks. Bacterial isolates were cultured in nutrient broth at 28 ± 2°C for 24 h on a rotary shaker (180 rpm) and standardised to ~ 10^8 CFU mL^{-1}. Cassava setts were primed with bacterial suspensions for 30 min and planted in pots containing 2 kg autoclaved soil amended with farmyard manure (50:1), followed by a 200 mL soil drench. The experiment was conducted in a completely randomised design with 10 replications using 15–20 cm stem cuttings containing six nodes. Pathogen challenge treatments received *F. falciforme* inoculum incorporated into the soil–FYM mixture at a 1:10 ratio before planting (Subhash et al., 2025), with carbendazim (50% WP at 0.1%) and uninoculated controls included for comparison. Disease incidence, including collar rot and wilt symptoms, was monitored periodically, and plant growth parameters such as plant height, leaf number, shoot and root biomass, root number, and root length were recorded at harvest to assess disease suppression and plant growth-promoting potential of the bacterial isolates.

Results

Sequencing Output, Diversity Metrics, and Microbial Community Structure Across Rhizoplane Agroecosystems

High-throughput 16S rRNA gene sequencing generated 4,374,469 (ULB), 5,151,637 (WDB), and 5,083,508 (WHB) raw sequences (Supplementary Table 1**)**. After quality filtering, 4,348,801, 5,488,413, and 5,055,496 high-quality reads were retained, respectively. GC content was consistent across groups (54.67–54.83%). Clustering produced 2,708 OTUs representing 1,431 bacterial genera. Rarefaction curves reached saturation, and coverage exceeded 99.9% in all libraries, confirming adequate sequencing depth despite variation in per-sample read counts (58,532–141,111) (Supplementary Fig. 1). WHB samples showed high richness with low inter-replicate variation, indicating a stable bacterial community. In contrast, WDB samples exhibited greater richness variability, suggesting disease-associated community disturbance. ULB samples exhibited lower richness, reflecting a more restricted yet distinct rhizoplane bacteriome associated with upland conditions.

Rhizoplane Community Structure/Microbial Abundance

Amplicon sequencing revealed distinct differences in cassava rhizoplane bacterial communities among upland (ULB), diseased wetland (WDB), and healthy wetland (WHB) agroecosystems (Fig. 1). At the phylum level, Pseudomonadota dominated all samples (65–90%). WHB harboured higher proportions of Bacteroidota (7.9%), Planctomycetota(5.7%), Actinomycetota(5.0%), and Acidobacteriota(3.0%), whereas WDB showed increased Verrucomicrobiota(7.35%) and reduced Bacteroidota (2.4%). ULB was enriched in Bacteroidota(9.5%) and Planctomycetota (8.6%) but contained lower Acidobacteriota(0.4%) (Fig. 1a). At the family level, Enterobacteriaceae remained abundant in WHB (15.2%) and WDB (17.1%). WHB was further characterised by Coxiellaceae(8.0%),Burkholderiaceae(4.5%), Bruguieriovoracaceae(4.4%),andXanthobacteriaceae(4.0%),while WDB showed enrichment ofAeromonadaceae(5.7%) andDevosiaceae(2.7%). In contrast, ULB was dominated by Pseudomonadaceae (29.8%), with lower abundances of Enterobacteriaceae(9.2%), Burkholderiaceae(4.5%), and Coxiellaceae (2.7%) (Fig. 1b). At the genus level, WHB supported a relatively balanced community comprising *Aquicella* (7.9%), *Chryseobacterium* (6.3%), *Sodalis* (4.4%), and *Enterobacter* (3.7%). WDB was characterised by increased abundances of *Aeromonas* (5.7%), *Salmonella* (5.0%), *Devosia* (2.6%), and Verrucomicrobia-associated taxa. In contrast, ULB was strongly enriched in *Pseudomonas* (29.7%), along with *Chryseobacterium* (3.8%) and *Sphingobacterium* (3.3%) (Fig. 1c). Similar agroecosystem-specific patterns were observed at the class and order levels, where the dominant bacterial lineages exhibited clear differences in relative abundance among the three habitats (Supplementary Figs. 2

and 3, respectively) collectively. However, a Pseudomonadota-dominated core microbiome was conserved across all rhizoplanes, agroecosystem and disease status substantially shaped community composition, with Aeromonadaceae, Devosiaceae, and Verrucomicrobiota associated with diseased wetlands and Pseudomonadaceae/*Pseudomonas* characteristic of upland rhizoplanes.

[Insert Fig. 1]

Alpha and Beta Diversity of the Cassava Rhizoplane Microbiome

Alpha- and beta-diversity analyses showed that the agroecosystem had a greater influence on cassava rhizoplane bacterial communities than plant health status (Fig. 2). Richness differed significantly among the three groups, with both the ACE and Chao 1 indices showing clear variation ($p = 0.0008$ and $p = 0.0025$, respectively). Diseased wetland samples (WDB) exhibited the highest richness (Chao 1 = 601. 60 ± 10. 10.37), followed by healthy wetland samples (WHB; 581. 20 ± 14. 39), whereas upland samples (ULB) had significantly lower richness (547. 97 ± 5. 74; $p < 0. 05$). In contrast, diversity and evenness metrics were comparable among groups, with no significant differences in Shannon ($p = 0. 434$) or Simpson ($p = 0. 448$) indices. Nevertheless, WDB samples consistently showed slightly higher Shannon diversity, while Simpson values were high in both wetland groups (0.96–0.97) but lower in ULB (0.83 ± 0.25), indicating greater taxonomic dominance in upland rhizoplanes. The beta- diversity analysis supported these observations. NMDS ordination based on Bray–Curtis dissimilarity produced an excellent two-dimensional representation of the data (stress = 0.0447) and revealed an agroecosystem-associated gradient in community composition. ULB samples clustered predominantly along the positive side of the NMDS 1 axis, whereas both WHB and WDB samples occupied the negative side. The substantial overlap between healthy and diseased wetland communities indicates that environmental conditions associated with wetland agroecosystems exert a stronger influence on bacterial community structure than plant health status. WHB samples formed the most compact cluster, suggesting a relatively stable and homogeneous bacterial assemblage, while WDB and ULB samples were more dispersed, reflecting greater variability in community composition. Despite these visual patterns, PERMANOVA detected no significant differences in overall community structure among the three groups ($F = 1.229$, $R^2 = 0.291$, $p = 0.192$). However, agroecosystem and health status together explained approximately 29% of the observed variation.

[Insert Fig. 2]

Core Microbiome of Cassava Rhizoplane

Analysis of the cassava rhizoplane bacteriome (n = 9) revealed a small but persistent core microbiome within a large accessory community (Fig. 3). Of the 638 taxa detected, no taxon occurred in all samples; however, *Aquicella, Escherichia, Klebsiella, Saccharimonas, Salmonella*, and *Sodalis* were present in 88.9% of samples (8/9), representing the most stable core members. At a prevalence threshold of ≥ 77.8% (7/9 samples), the core community also included *Devosia, Enterobacter*, and *Nanosynbacter*, while a threshold of ≥ 55.6% (5/9 samples) expanded the core to 19 genera. Across relative abundance thresholds, *Aquicella, Salmonella, Sodalis, Saccharimonas*, and *Klebsiella* remained consistently prevalent, whereas *Pseudomonas* persisted even at the highest abundance threshold, indicating both widespread occurrence and high abundance.

[Insert Fig. 3]

Other persistent genera included *Chryseobacterium, Sphingobacterium*, and *Aeromonas*, while *Sphingomonas, Limnoglobus*, and *Gemmata* were infrequent and restricted to a subset of samples. Overall, the rhizoplane microbiome was structured around a conserved core dominated by Enterobacteriaceae-associated genera and key taxa such as *Aquicella, Sodalis*, and *Pseudomonas*. In contrast, approximately 92% of detected taxa occurred in fewer than half of the samples, forming a diverse accessory bacteriome that contributed to agroecosystem- and host-associated variation. Core microbiome analysis further identified distinct sets of persistent bacterial taxa associated with upland eubiosis, wetland dysbiosis, and wetland eubiosis states (Supplementary Figs. 4–6).

Shared Taxa

OTU distribution across Wetland Healthy (WHB), Wetland Diseased (WDB), and Upland (ULB) rhizoplane samples (n = 9) revealed both a conserved core bacteriome and agroecosystem-specific communities. UpSet analysis identified 1,079 OTUs shared among all groups, representing 39.8% of the 2,708 detected OTUs and constituting the core cassava rhizoplane bacteriome (Supplementary Fig. 7). Agroecosystem-specific taxa were most abundant in WDB (384 OTUs; 14.2%) and ULB (328 OTUs; 12.1%), whereas WHB contained fewer unique OTUs (227 OTUs; 8.4%). Pairwise overlaps were greatest between the wetland groups (WHB–WDB: 360 OTUs; 13.3%), compared with WDB–ULB (212 OTUs; 7.8%) and WHB–ULB (118 OTUs; 4.4%). These patterns indicate greater similarity between wetland bacterial communities and support the agroecosystem-associated clustering observed in the beta-diversity analysis.

Co-occurrence Analysis and Identification of Hub Taxa

Inter-kingdom co-occurrence network analysis based on Spearman correlations ($|r| \geq 0.5$, $P < 0.05$; FDR-corrected) revealed a highly structured microbial network comprising both positive and negative interactions between bacterial and fungal taxa (Fig. 4). The network displayed extensive cross-kingdom connectivity, with fungal families Geminigeraceae, Glomerellaceae, and Mycosphaerellaceae, and bacterial families Hyphomonadaceae and Desulfitobacteriaceae, identified as major hub taxa. Among these, Geminigeraceae emerged as a potential keystone taxon due to its central position and broad connectivity. Betweenness and closeness centrality analyses further identified taxa with potentially important roles in network connectivity and community organisation within the cassava rhizoplane microbiome (Supplementary Fig. 8). Positive interactions predominated throughout the network, particularly among Mycosphaerellaceae and Glomerellaceae, which exhibited numerous associations with diverse bacterial taxa. In contrast, Schizosaccharomycetaceae served as a major negative hub, exhibiting antagonistic interactions with several bacterial families, including Steroidobacteriaceae, Eubacteriaceae, and Sirenicapillariaceae. Other fungal groups, such as Didymellaceae and Glomerellaceae, exhibited both positive

and negative associations, indicating context-dependent ecological roles. Collectively, the network suggests that cooperative interactions dominate the cassava rhizoplane microbiome, while specific antagonistic relationships may contribute to microbial recruitment and community assembly.

[Insert Fig. 4]

Culture-based Validation of mNGS-Derived OTUs

Culture-based isolation and 16S rRNA gene sequencing were used to validate OTUs identified by mNGS across three cassava rhizoplane habitats. A total of 195 bacterial isolates were recovered, comprising 54 from Upland (ULB), 74 from Wetland Diseased (WDB), and 67 from Wetland Healthy (WHB) samples. The cultured isolates largely matched the dominant taxa detected by metabarcoding, confirming the reliability of the mNGS-derived community profiles (Table 1). A total of 23 bacterial genera were identified, with *Enterobacter*, *Klebsiella*, *Kosakonia*, and *Pseudomonas* comprising the core microbiome. ULB samples were characterised by *Enterobacter* (9 isolates), *Klebsiella* (7), and *Bacillus* (5), whereas WDB samples were dominated by *Enterobacter* (24), *Kosakonia* (12), and *Klebsiella* (10). Similarly, WHB samples were dominated by *Enterobacter* (21), *Klebsiella* (9), and *Kosakonia* (8). Core genera shared across agroecosystems included *Enterobacter*, *Klebsiella*, *Kluyvera*, *Kosakonia*, *Pseudomonas*, and *Stenotrophomonas*. Several beneficial taxa, including *Bacillus*, *Pseudomonas*, *Priestia*, and *Rhizobium*, were more prevalent in upland and healthy wetland rhizoplanes. *Pseudomonas* exhibited the greatest diversity in ULB, whereas *Bacillus* exhibited the greatest diversity in WHB. In contrast, WDB communities were characterised by the predominance of *Enterobacter* and *Kosakonia*, along with reduced diversity of beneficial bacterial taxa, consistent with shifts observed in the sequencing-based community analyses.

Table 1
Distribution of bacterial taxa in the cassava rhizoplane across three microhabitats of cassava

*Bacterial Genus	Upland non-endemic cassava agroecosystem	Wetland Diseased	Wetland Healthy	**Core Microbiome
*Acinetobacter***(6)**	—	*Acinetobacter nosocomialis*(2), *Acinetobacter pittii*(1), *Acinetobacter* sp.(1) (PZ008117, PZ008118, PZ008107, PZ008162)	*Acinetobacter pittii*(2) (PZ028150, PZ028134)	**Yes**
*Aeromonas***(4)**	—	*Aeromonas hydrophila*(1), *Aeromonas media* (1), *Aeromonas* sp. (2) (PZ008159, PZ008126, PZ008119, PZ008124)	—	**Yes**
*Bacillus***(7)**	*Bacillaceaebacterium*(1), *Bacillus aerophilus*(1), *Bacillus pumilus*(1), *Bacillus stercoris*(1), *Bacillus subtilis* (1) (PZ094595, PZ094637, PZ094615, PZ094603, PZ094624)	*Bacillus infantis* (1), *Bacillus* sp.(1) (PZ008101, PZ008115)	—	**Yes**
*Burkholderia***(2)**	*Burkholderiacenocepacia*(1),*Burkholderia*sp. (1) (PZ094630, PZ094612)	—	—	**Yes**
*Chitinophaga***(1)**	*Chitinophaga*sp.(1) (PZ094645)	—	—	**Yes**
*Chryseobacterium***(3)**	—	*Chryseobacterium*sp. (3) (PZ008156, PZ008157, PZ008160)	—	**Yes**
Citrobacter **(7)**	*Citrobacter freundii* (1), *Citrobacter werkmanii* (1) (PZ094641, PZ094601)	*Citrobacter amalonaticus* (1), *Citrobacter farmeri* (2), *Citrobacter* sp. (1) (PZ008133, PZ008110, PZ008138, PZ008099)	*Citrobacter* sp. (1) (PZ028148)	**Yes**
*Cupriavidus***(1)**	*Cupriavidus*sp.(1) (PZ094610)	—	—	**Yes**
*Cytobacillus***(6)**	*Cytobacillus firmus* (1), *Cytobacilluskochii* (1) (PZ094594, PZ094600)	*Cytobacilluskochii* (1) (PZ008106)	*Cytobacillusoceanisediminis* (3) (PZ028132, PZ028137, PZ028159)	**Yes**
*Ensifer***(1)**	*Ensifer*sp.(1) (PZ094617)	—	—	**No**
Enterobacter **(54)**	*Enterobacter cloacae* (3), *Enterobacter pseudoroggenkampii*(1), *Enterobacter* sp. (5) (PZ094607, PZ094626, PZ094628, PZ094642, PZ094596, PZ094620, PZ094629, PZ094636, PZ094639)	*Enterobacter chengduensis*(2), *Enterobacter cloacae* (1), *Enterobacter hormaechei*(3), *Enterobacter kobei*(1), *Enterobacter sichuanensis (1)*, *Enterobacter soli* (4), *Enterobacter* sp. (12) (PZ008112, PZ008103, PZ008143, PZ008116, PZ008109, PZ008098, PZ008113, PZ008139, PZ008123, PZ008134, PZ008137, PZ008167, PZ008100, PZ008108, PZ008114, PZ008125, PZ008132, PZ008135, PZ008146, PZ008152, PZ008154, PZ008131, PZ008151, PZ008155)	*Enterobacter huaxiensis*(3), *Enterobacter* sp. (18) (PZ028152, PZ028165, PZ028169, PZ028130, PZ028135, PZ028138, PZ028147, PZ028155, PZ028163, PZ028164, PZ028171, PZ028172, PZ028174, PZ028175, PZ028177, PZ028180, PZ028181, PZ028186, PZ028187, PZ028188, PZ028190)	**Yes**
*Epilithonimonas***(1)**	—	—	*Epilithonimonasarachidiradicis*(1) (PZ028158)	**No**
*Falsibacillus***(1)**	—	—	*Falsibacillus*sp. (1) (PZ028143)	**No**
Klebsiella **(26)**	*Klebsiella aerogenes* (4), *Klebsiella* sp. (3) (PZ094602, PZ094625, PZ094627, PZ094638, PZ094619, PZ094622, PZ094623)	*Klebsiella aerogenes* (4), *Klebsiella quasivariicola*(3), *Klebsiella* sp. (1), *Klebsiella variicola* (2) (PZ008102, PZ008104, PZ008111,	*Klebsiella aerogenes* (1), *Klebsiella pneumoniae* (1), *Klebsiella* sp. (7) (PZ028156, PZ028193, PZ028141, PZ028144, PZ028178,	**Yes**

Figures in parentheses indicate the number of genera or species. *A 1350 bp sequence length obtained by 16S rRNA gene sequencing was used to identify bacteria at the species level; All sequences have been submitted to GenBank (https://www.ncbi.nlm.nih.gov/nucleotide/); **The isolated genera were compared with the core microbiome data determined through metabarcoding.
Note: The linkage between isolate-derived 16S rRNA gene sequences and OTUs was based on taxonomic assignments by closest match. Although generated using different sequencing approaches with varying read lengths, both datasets represent the 16S rRNA gene marker widely used for bacterial identification and species delineation. This integration enabled functional validation of representative microbial taxa detected through amplicon sequencing.

*Bacterial Genus	Upland non-endemic cassava agroecosystem	Wetland Diseased	Wetland Healthy	**Core Microbiome
		PZ008127, PZ008122, PZ008161, PZ008163, PZ008170, PZ008129, PZ008140)	PZ028179, PZ028182, PZ028184, PZ028189)	
*Kluyvera***(9)**	*Kluyveracryocrescens*(1), *Kluyvera*sp. (1) (PZ094640, PZ094597)	*Kluyverageorgiana*(1), *Kluyvera*sp. (2) (PZ008141, PZ008168, PZ008150)	*Kluyverageorgiana* (1), *Kluyvera*sp. (3) (PZ028166, PZ028146, PZ028151, PZ028170)	**Yes**
*Kosakonia***(20)**	—	*Kosakoniaoryzendophytica*(4), *Kosakoniapseudosacchari* (5), *Kosakonia*sp.(3) (PZ008142, PZ008149, PZ008153, PZ008164, PZ008144, PZ008147, PZ008148, PZ008165, PZ008169, PZ008130, PZ008136, PZ008145)	*Kosakoniapseudosacchari* (2), *Kosakonia*sp.(6) (PZ028168, PZ028133, PZ028149, PZ028154, PZ028157, PZ028167, PZ028173, PZ028191)	**Yes**
*Kytococcus***(1)**	*Kytococcussedentarius*(1) (PZ094613)	—	—	**No**
*Leclercia***(2)**	—	—	*Leclercia*sp.(1), *Leclerciatamurae* (1) (PZ028153, PZ028160)	**Yes**
*Lysinibacillus***(1)**	*Lysinibacillus*sp.(1) (PZ094635)	—	—	**Yes**
*Neobacillus***(1)**	*Neobacillusdrentensis*(1) (PZ094605)	—	—	**Yes**
*Niallia***(4)**	*Nialliacirculans*(1) (PZ094598)	—	*Niallia*sp. (3) (PZ028139, PZ028145, PZ028192)	**No**
*Novosphingobium***(1)**	—	—	*Novosphingobiumpanipatense* (1) (PZ028161)	**Yes**
*Pantoea***(3)**	—	*Pantoeadispersa*(1) (PZ008166)	*Pantoeadispersa*(2) (PZ028176, PZ028185)	**Yes**
*Phytobacter***(2)**	—	*Phytobacterdiazotrophicus*(2) (PZ008120, PZ008128)	—	**Yes**
*Priestia***(3)**	*Priestiaaryabhattai*(1) (PZ094608)	—	*Priestia*sp.(2) (PZ028140, PZ028142)	**Yes**
Pseudomonas **(11)**	*Pseudomonas aeruginosa* (1), *Pseudomonas nicosulfuronedens*(1), *Pseudomonas* sp. (2) (PZ094604, PZ094599, PZ094621, PZ094646)	*Pseudomonas knackmussii*(1), *Pseudomonas oleovorans*(1) (PZ008171, PZ008158)	*Pseudomonas alloputida*(1), *Pseudomonas kurunegalensis*(1), *Pseudomonas* sp. (2), *Pseudomonas wayambapalatensis* (1) (PZ028183, PZ028162, PZ028195, PZ028196, PZ028194)	**Yes**
*Ralstonia***(1)**	*Ralstonia soli* (1) (PZ094631)	—	—	**Yes**
Rhizobium **(2)**	*Rhizobium dioscoreae*(2) (PZ094632, PZ094644)	—	—	**Yes**
Salmonella **(1)**	*Salmonella* sp.(1) (PZ094618)	—	—	**Yes**
Staphylococcus **(4)**	*Staphylococcus arlettae*(1), *Staphylococcus hominis* (1), *Staphylococcus saprophyticus* (1), *Staphylococcus warneri*(1) (PZ094614, PZ094606, PZ094616, PZ094611)	—	—	**Yes**
Stenotrophomonas **(4)**	*Stenotrophomonas* sp.(1) (PZ094609)	*Stenotrophomonas* sp.(1) (PZ008121)	*Stenotrophomonas maltophilia*(1), *Stenotrophomonas* sp.(1) (PZ028136, PZ028131)	**Yes**
*Stutzerimonas***(1)**	—	*Stutzerimonasstutzeri*(1) (PZ008105)	—	**Yes**
*Sutcliffiella***(1)**	*Sutcliffiella*sp. (1) (PZ094593)	—	—	**No**
*Variovorax***(3)**	*Variovoraxguangxiensis*(3) (PZ094633, PZ094634, PZ094643)	—	—	**Yes**

Figures in parentheses indicate the number of genera or species. *A 1350 bp sequence length obtained by 16S rRNA gene sequencing was used to identify bacteria at the species level; All sequences have been submitted to GenBank (https://www.ncbi.nlm.nih.gov/nucleotide/); **The isolated genera were compared with the core microbiome data determined through metabarcoding.
Note: The linkage between isolate-derived 16S rRNA gene sequences and OTUs was based on taxonomic assignments by closest match. Although generated using different sequencing approaches with varying read lengths, both datasets represent the 16S rRNA gene marker widely used for bacterial identification and species delineation. This integration enabled functional validation of representative microbial taxa detected through amplicon sequencing.

*Bacterial Genus	Upland non-endemic cassava agroecosystem	Wetland Diseased	Wetland Healthy	**Core Microbiome
Total-195	**54**	**74**	**67**	

Figures in parentheses indicate the number of genera or species. *A 1350 bp sequence length obtained by 16S rRNA gene sequencing was used to identify bacteria at the species level; All sequences have been submitted to GenBank (https://www.ncbi.nlm.nih.gov/nucleotide/); **The isolated genera were compared with the core microbiome data determined through metabarcoding.
Note: The linkage between isolate-derived 16S rRNA gene sequences and OTUs was based on taxonomic assignments by closest match. Although generated using different sequencing approaches with varying read lengths, both datasets represent the 16S rRNA gene marker widely used for bacterial identification and species delineation. This integration enabled functional validation of representative microbial taxa detected through amplicon sequencing.

[Insert Table 1]

Screening of Culturable Rhizoplane Bacterial Isolates against Fusarium falciforme

To evaluate the functional potential of the culturable rhizoplane bacteriome, isolates were screened for antifungal activity against *Fusarium falciform*e using dual-culture and volatile-inhibition assays.

Dual Culture Antagonism

In the dual culture assay, which measures contact-dependent antagonism through competition or the production of diffusible metabolites, the Upland (ULB) agroecosystem yielded the most potent antagonists, led by *Bacillus subtilis* ULB_36 (83.33% PI) and *Bacillus stercoris* ULB_12 (78.52% PI) (Table 2; Supplementary Fig. 9). These were followed by *Pseudomonas aeruginosa* ULB_13 (61.48% PI) and *Bacillus aerophilus* ULB_53 (59.26% PI). In the Wetland Healthy (WHB) agroecosystem, direct inhibition was primarily driven by *Acinetobacter* sp. WHB_6 (60.37% PI) and *Kosakonia* sp.7 WHB_75 (60.00% PI). In contrast, the Wetland Diseased (WDB) agroecosystem exhibited lower overall direct activity, with the highest inhibition observed *against Bacillus* sp. WDB_25 (52.96% PI) and *Kosakonia* sp.1 WDB_41 (51.11% PI).In addition to the highly inhibitory strains described above, several isolates showed moderate to low antagonistic activity (< 50% PI), the details of which are provided in Supplementary Table 2.

Table 2
Secreted metabolome-mediated antifungal activity of rhizoplane bacterial isolates recovered from stem androot rot-endemic and non-endemic cassava agroecosystems

Isolate	Mycelial Inhibition (%)
Upland non-endemic cassava agroecosystem	
Bacillus subtilis ULB-36	83.33 ± 0.00[a]
Bacillus stercoris ULB-12	78.52 ± 0.64[b]
Pseudomonas aeruginosa ULB-13	61.48 ± 1.70[c]
Bacillus aerophilus ULB-53	59.26 ± 1.70[c]
Bacillus pumilus ULB-25	59.26 ± 1.70[c]
Enterobacter sp.2 ULB-31	53.70 ± 1.70[d]
*Klebsiella aerogenes*3 ULB-39	52.96 ± 1.28[de]
Burkholderiacenocepacia ULB-43	52.59 ± 2.80[de]
Pseudomonas sp.1 ULB-33	52.59 ± 2.80[de]
Stenotrophomonas sp. ULB-18	51.11 ± 2.94[e]
*Burkholderia*sp. ULB-22	50.74 ± 0.64[e]
Enterobacter cloacae 2 ULB-38	50.74 ± 1.28[e]
Wetland disease-endemic cassava agroecosystem (Diseased plants)	
Bacillus sp. WDB-25	52.96 ± 0.64[a]
*Kosakonia*sp.1 WDB-41	51.11 ± 1.92[ab]
*Kosakonia*sp.3 WDB-58	51.11 ± 1.11[ab]
*Kosakonia pseudosacchari*4 WDB-78	50.00 ± 0.00[bc]
Stenotrophomonas sp. WDB-31	50.00 ± 0.00[bc]
Wetland disease-endemic cassava agroecosystem (Healthy plants)	
*Acinetobacter pittii*WHB-6	60.37 ± 1.28[a]
*Kosakonia*sp.7WHB-75	60.00 ± 1.11[a]
*Kosakonia pseudosacchari*WHB-4	55.56 ± 0.00[b]
*Klebsiella pneumoniae*WHB-81	54.81 ± 1.28[b]
*Priestia*sp.1WHB-14	52.22 ± 1.11[c]
Klebsiella sp.3WHB-57	50.00 ± 1.11[c]
Klebsiella sp.5WHB-64	50.00 ± 1.11[c]

Note: ULB = upland non-endemic cassava agroecosystem; WDB = wetland disease-endemic cassava agroecosystem (diseased plants); WHB = wetland disease-endemic cassava agroecosystem (healthy plants). *Fusarium falciforme*was used as the target pathogen in the dual-culture assay. Values represent per cent inhibition (PI, mean ± SD; n = 3). Different lowercase letters within each habitat indicate significant differences among isolates according to ANOVA

[Insert Table 2]

Volatile Organic Compound (VOC) Inhibition Assay

Non-contact antagonism mediated by volatile organic compounds (VOCs) was a major contributor to fungal suppression across all agroecosystems (Table 3; Supplementary Fig. 10). The highest VOC-mediated inhibition was observed in the Upland isolate *Nialliacirculans* ULB_7 (69.63% PI), followed by the

healthy wetland isolate *Klebsiella pneumoniae* WHB_81 (64.44% PI) and the diseased wetland isolate *Pseudomonasknackmussii*WDB_84 (61.85% PI). Other notable VOC producers included *Pseudomonas* sp.1 WHB_83 (60.37% PI), *Bacillus infantis* WDB_4 (59.26% PI), *Pseudomonas* sp.1 ULB_33 (58.52% PI), and *Pseudomonas alloputida* WHB_65 (56.30% PI). The remaining isolates displayed comparatively lower volatile-mediated antifungal activity (< 50% PI) and are summarised in Supplementary Table 3.

Table 3
Volatile inhibition-mediatedantifungal activity of rhizoplane bacterial isolates recovered from stem and root rot-endemic and non-endemic cassava agroecosystems

Isolate	**Mycelial Inhibition (%)**
Upland non-endemic cassava agroecosystem	
Nialliacirculans ULB-7	69.63 ± 2.31[a]
Pseudomonas sp.1 ULB-33	58.52 ± 0.64[b]
Bacillus subtilis ULB-36	55.56 ± 0.00[c]
Bacillus pumilus ULB-25	52.59 ± 2.80[d]
Pseudomonas aeruginosa ULB-13	51.48 ± 1.28[de]
Priestiaaryabhattai ULB-17	50.37 ± 0.64[def]
Wetland disease-endemic cassava agroecosystem (Diseased plants)	
*Pseudomonas knackmussii*WDB-84	61.85 ± 0.64[a]
Bacillus infantis WDB-4	59.26 ± 1.28[b]
Stutzerimonasstutzeri WDB-11	53.70 ± 0.64[c]
Cytobacilluskochii WDB-12	50.74 ± 0.64[d]
Pseudomonas oleovorans WDB-71	50.00 ± 1.11[d]
Wetland disease-endemic cassava agroecosystem (Healthy plants)	
*Klebsiella pneumoniae*WHB-81	64.44 ± 1.11[a]
Pseudomonas sp.1WHB-83	60.37 ± 0.64[b]
*Pseudomonas alloputida*WHB-65	56.30 ± 0.64[c]
Stenotrophomonas sp.1WHB-2	56.30 ± 0.64[c]
*Pantoea dispersa*1WHB-55	55.19 ± 0.64[c]
*Kosakonia pseudosaccharii*WHB-4	54.81 ± 1.28[c]
*Stenotrophomonas maltophilia*WHB-8	54.81 ± 0.64[c]
*Cytobacillus oceanisediminis*3WHB-35	54.07 ± 0.64[c]
*Pantoea dispersa*2WHB-67	50.00 ± 1.92[d]

ULB = upland non-endemic cassava agroecosystem; WDB = wetland disease-endemic cassava agroecosystem (diseased plants); WHB = wetland disease-endemic cassava agroecosystem (healthy plants). *Fusarium falciforme*was used as the target pathogen in the Volatile Assay. Values represent per cent inhibition (PI, mean ± SD; n = 3). Different lowercase letters within each agroecosystem indicate significant differences among isolates according to ANOVA

[Insert Table 3]

Cumulative Antagonistic Potential

The upland bacteriome exhibited superior antagonistic potential, with *Bacillus subtilis* ULB_36 at 69.44% and *Bacillus stercoris* ULB_12 at 63.15% (Supplementary Table 4). In healthy wetlands, *Klebsiella pneumoniae* WHB_81 (59.63%) was the top antagonist, whereas *Pseudomonas knackmussii* WDB_84 (53.15%) was most effective in diseased rhizoplanes.

In-Planta Evaluation of Antagonistic Bacterial Isolates for Disease Suppression

Suppression of Disease Incidence

The efficacy of bacterial isolates against stem and root rot in cassava was assessed using Percentage Disease Incidence (PDI). The control showed the highest infection at 70% PDI. *Bacillus subtilis* ULB_36 achieved complete suppression, with a PDI of 0%, comparable to the healthy control (Fig. 5). *Bacillus stercoris* ULB_129 also provided notable protection, reducing disease to 20%. *B. subtilis* ULB_36 was as effective as the chemical control (Carbendazim 50% WP – 0.1%), which also recorded 0%. These results highlight strain ULB_36 as a highly protective bacterial antagonist against *Fusarium falciforme* under greenhouse conditions.

[Insert Fig. 5]

Biocontrol Efficacy and Plant Growth Promotion

The greenhouse trial confirmed that *B. subtilis* ULB_36 and *Bacillus stercoris* ULB_12 retained their inhibitory effects in the rhizosphere. ULB_36 was the most effective, outperforming controls in plant height (71.97 cm), shoot weight (31.87 g), and root weight (2.48 g)(Supplementary Table 5). *Bacillus stercoris* ULB_12 showed improved growth relative to the pathogen-inoculated control but was less effective than ULB_36 (53.02 cm in height). Pathogen-inoculated plants exhibited severe symptoms, including growth retardation and root decay. ULB_36 significantly increased root number (29.60) and sett weight (79.23 g), underscoring its potential as a biocontrol agent and plant growth promoter against cassava stem and root rot.

Discussion

Cassava production is increasingly threatened by soil-borne diseases, particularly stem and root rot by *Fusarium*, which reduces root yield and the quality of planting material. Although plant-associated microbiomes are increasingly recognised as key determinants of plant health and disease suppression, the ecological mechanisms governing rhizoplane microbial assembly across contrasting production systems remain poorly understood. By integrating culture-independent and culture-dependent approaches, this study examined how agroecosystem and disease shape the cassava rhizoplane microbiome and identified microbial taxa with potential biocontrol activity. The high sequencing depth, reflected in coverage values exceeding 99.9% and saturated rarefaction curves, ensured robust representation of bacterial diversity. The detection of 2,708 OTUs and 1,431 genera further demonstrates the remarkable complexity of the cassava rhizoplane microbiome. It indicates that the observed differences among agroecosystems reflect genuine ecological variation rather than sampling artefacts (Liao et al. 2026).

Across all agrosystems, Pseudomonadota dominated the bacterial community, indicating a conserved functional core microbiome. Members of this phylum are renowned for their metabolic versatility, ecological adaptability, and ability to colonise diverse plant-associated environments (Turner et al. 2013; Trivedi et al. 2020). A similar dominance of Pseudomonadaceae has been reported in cassava-associated microbiomes across a range of agroecological settings (Ha et al. 2021; Zhang et al. 2021). Despite the stability of this core component, substantial variation was observed in the accessory microbiome. Healthy wetland rhizoplanes were enriched in Bacteroidota, Planctomycetota, and Actinomycetota, taxa commonly associated with organic matter degradation and nutrient cycling in saturated soils. In contrast, upland rhizoplanes showed marked enrichment of *Pseudomonas*, reflecting adaptation to lower soil moisture and greater oxygen availability, as well as the well-established roles of this genus in producing antimicrobial metabolites and inducing systemic resistance in plants (Raaijmakers et al. 2009; Latz et al. 2012).

Disease was associated with pronounced changes in microbiome composition. Diseased wetland rhizoplanes showed increased abundance of Verrucomicrobiota and opportunistic genera such as *Aeromonas* and *Salmonella*, alongside a decline in potentially beneficial taxa, indicating microbial dysbiosis. Similar disease-associated shifts have been reported in cassava and other crop systems, where pathogen invasion disrupts resident microbial communities and alters ecological interactions (Zeng et al. 2021; Zapata et al. 2021). The depletion of beneficial groups, particularly members of Bacteroidota, may reduce functional redundancy and resilience, thereby increasing vulnerability to pathogen establishment. Conversely, the relative stability of healthy rhizoplane communities suggests that microbiome integrity contributes to natural disease suppression.

Patterns of alpha diversity further support this interpretation. Diseased wetland rhizoplanes exhibited the highest species richness, whereas diversity and evenness remained comparatively stable across agroecosystems. This pattern suggests that disease facilitates the recruitment or proliferation of rare and opportunistic taxa without substantially altering dominant community members. Increased richness under stress is consistent with ecological disturbance and niche expansion, whereby newly available ecological opportunities permit colonisation by additional taxa (van der Heijden and Hartmann 2016). Importantly, the greater diversity observed in wetland systems indicates that diversity alone is insufficient to confer disease resistance; rather, the taxonomic composition and functional attributes of microbial communities appear to be more important determinants of plant health.

Beta diversity analyses reinforced the dominant influence of the agroecosystem on microbial assembly. The clear separation between upland and wetland communities indicates strong environmental filtering driven by differences in soil moisture and associated edaphic conditions. In contrast, healthy and diseased wetland communities showed substantial overlap, suggesting that disease effects operate within the constraints of the agroecosystem. Similar observations have been reported in cassava systems, where environmental variables consistently outweigh host health status as drivers of microbiome composition (Huang et al. 2024; Somyong et al. 2025; Qi et al. 2025). Nevertheless, diseased wetland communities displayed greater dispersion, consistent with the Anna Karenina principle, which predicts that stressed microbiomes become increasingly variable and less predictable than their healthy counterparts (Zaneveld et al. 2017).

The identification of a conserved core microbiome comprising *Enterobacter*, *Klebsiella*, *Sodalis*, and *Aquicella* across all agroecosystems further supports the presence of stable microbial assemblages adapted to cassava roots. These taxa may play fundamental roles in root colonisation, nutrient acquisition, and plant–microbe interactions, consistent with previous reports of persistent cassava-associated bacterial lineages across diverse geographic regions

and host genotypes (Ha et al. 2021). In contrast, the accessory microbiome, which comprises more than 90% of detected taxa, showed strong agroecosystem responsiveness, supporting contemporary models in which microbiome resilience arises from interactions between a stable core and a dynamic accessory component (Vandenkoornhuyse et al. 2015; Toju et al. 2018).

Network analysis provided further insight into the ecological organisation of the rhizoplane microbiome. The highly interconnected network structure suggests extensive microbial interactions within cassava roots. Fungal families such as Geminigeraceae, Glomerellaceae, and Mycosphaerellaceae occupied central positions in the network, indicating potentially important roles in shaping community structure and interaction dynamics. The predominance of positive associations implies that cooperative relationships contribute substantially to community stability, whereas antagonistic hubs, including Schizosaccharomycetaceae, may regulate network organisation and prevent dominance by individual taxa. Such highly connected organisms are often regarded as keystone taxa that exert disproportionate influence on microbiome stability and ecosystem functioning (Agler et al. 2016; Banerjee et al. 2018).

Culture-dependent analyses largely corroborated the sequencing results. Genera such as *Enterobacter*, *Klebsiella*, *Kosakonia*, and *Pseudomonas* were consistently isolated across agroecosystems, confirming their ability to colonise cassava roots. Moreover, healthy and upland rhizoplanes harboured a broader diversity of beneficial bacterial taxa, including *Bacillus*, *Pseudomonas*, *Priestia*, and *Rhizobium*. In contrast, diseased rhizoplanes exhibited reduced culturable diversity, suggesting erosion of functional microbial capacity under disease pressure.

Functional screening further revealed that isolates from healthy and upland rhizoplanes generally exhibited stronger antagonistic activity against *Fusarium falciform*e than those from diseased plants. Among these, *Bacillus subtilis* displayed particularly strong antifungal activity, likely mediated by the production of antimicrobial lipopeptides such as surfactins, iturins, and fengycins (Ongena and Jacques 2008), as well as volatile organic compounds that suppress pathogen growth (Kai 2020; Owino et al. 2026). The reduced antagonistic potential observed among isolates from diseased rhizoplanes provides additional evidence that disease is associated with a loss of functional resilience within the microbial community.

The ecological relevance of these findings was confirmed under greenhouse conditions, where *Bacillus subtilis* ULB_36 significantly suppressed stem and root rot by *Fusarium*and enhanced cassava growth. These outcomes align with established mechanisms of *Bacillus*-mediated biocontrol, including antibiosis, efficient root colonisation, competition for ecological niches, and activation of plant defence responses (Ubalua et al. 2020; Saengchan et al. 2021, 2022). The strong performance of ULB_36 underscores the value of harnessing native microbiome members as sustainable alternatives to chemical disease management strategies (Nihorimbere et al. 2024).

Collectively, these findings show that the cassava rhizoplane microbiome is structured primarily by agroecosystem-driven environmental filtering and secondarily by disease status. While a stable core microbiome maintains ecological continuity across contrasting agroecosystems, disease is linked to reorganisation of the accessory microbiome, leading to microbial dysbiosis, increased community heterogeneity, depletion of beneficial taxa, and reduced antagonistic potential. The enrichment of opportunistic taxa such as *Aeromonas* and *Salmonella*, alongside the decline of functionally important groups, suggests that shifts in community composition may serve as early ecological indicators of disease development before severe symptoms appear. Importantly, the higher richness observed in diseased rhizoplanes indicates that microbiome resilience is determined not by diversity alone but by the maintenance of functionally coherent microbial assemblages. By integrating metabarcoding with culturomics, this study bridges ecological inference and functional validation, demonstrating that disease-suppressive potential is concentrated within specific members of the native microbiome. The identification of *Bacillus subtilis* ULB_36 as a highly effective antagonist of *Fusarium falciforme* highlights the promise of harnessing endemic rhizoplane bacteria for microbiome-informed disease management. These findings provide a conceptual framework for developing predictive microbiome biomarkers and next-generation biological control strategies to enhance cassava health, resilience, and productivity in disease-prone agroecosystems.

Conclusion

We analysed cassava rhizoplane microbial diversity and succession across contrasting agroecological habitats and health states affected by *Fusarium falciforme* by integrating 16S rRNA amplicon sequencing, culture-based validation, and functional assays. Microbial richness varied significantly among groups, with higher diversity observed under diseased wetland conditions due to increased turnover of rare taxa, while community evenness remained stable. A conserved core microbiome was maintained across agroecosystems, suggesting its role in rhizoplane functionality and disease resilience. Among the antagonistic isolates identified, the core members -*Bacillus subtilis* ULB_36 and *Bacillus stercoris* ULB_12 showed strong suppression of *F. falciforme*, with ULB_36 achieving complete disease control and promoting plant growth under greenhouse conditions. These findings demonstrate the potential of microbiome-based strategies for sustainable management of cassava stem and root rot disease.

Declarations

Metagenome data availability

SRA submission: Bio Project accession: PRJNA1433807

Author Contributions Statement

S. Divya conducted the investigation, data analysis, visualisation, and prepared the original draft. T.K. Bag and T. Makeshkumar contributed to conceptualisation, supervision, resource provision, and manuscript review and editing. M.L. Jeeva, Binoy Ambika Manirajan, Vinod Chouhan, and S.S. Veena contributed to the investigation, methodology, review and editing of the manuscript. Aundy Kumar conceived and supervised the study, provided technical expertise, administered the project, and contributed to manuscript review, editing, and critical revisions. All authors read and approved the final manuscript.

Declaration of Competing Interest

We, the authors of the research paper titled **Agroecosystem-Driven Rhizoplane Bacteriome Assembly in Cassava Uncovers Bacillus-Mediated Suppression of Stem and Root Rot**declare that there are no conflicts of interest related to the manuscript submitted to the journal.

Acknowledgment

We thank the Directors of ICAR-IARI, New Delhi, and ICAR-CTCRI, Thiruvananthapuram, for their support and encouragement. We would especially like to thank the Director of CTCRI for providing the laboratory facilities, which were essential to completing this work. Mrs. Divya S acknowledges Kerala Agricultural University for providing study leave for PhD work.

Funding Statement

The authors acknowledge the financial support provided by the Indian Council of Agricultural Research (ICAR), Department of Agricultural Research and Education (DARE), Government of India, for this research. Ms. Divya S gratefully acknowledges ICAR-CTCRI, Thiruvananthapuram, for providing financial assistance towards her PhD research project. Dr. Aundy Kumar acknowledges the funding support from the Flagship Project on *Functional Importance and Translational Applications of Microbiomes for Crop Productivity* at ICAR-IARI, New Delhi.

Ethical Statement

Our work and the manuscript **on Agroecosystem-Driven Rhizoplane Bacteriome Assembly in Cassava Uncovers *Bacillus*-Mediated Suppression of Stem and Root Rot** complies with the journal's Ethical Rules.

Declaration of generative A.I. and AI-assisted technologies in the writing process

While preparing this work, we used Grammarly and ChatGPT to improve the language. After using this tool/service, we reviewed and edited the content as needed and took full responsibility for the publication's content

References

1. Agler MT, Ruhe J, Kroll S, et al (2016) Microbial Hub Taxa Link Host and Abiotic Factors to Plant Microbiome Variation.PLoSBiol14:e1002352. https://doi.org/10.1371/journal.pbio.1002352
2. Banerjee S, Schlaeppi K, van der Heijden MGA (2018) Keystone taxa as drivers of microbiome structure and functioning. Nat Rev Microbiol 16:567–576. https://doi.org/10.1038/s41579-018-0024-1
3. Busby PE, Soman C, Wagner MR, et al (2017) Research priorities for harnessing plant microbiomes in sustainable agriculture. PLoSBiol15:e2001793. https://doi.org/10.1371/journal.pbio.2001793
4. Chen S, Zhou Y, Chen Y, Gu J (2018). Fastp: an ultra-fast all-in-one FASTQ preprocessor. Bioinformatics 34:i884–i890. https://doi.org/10.1093/bioinformatics/bty560
5. da Silva JSA, da Silva Santos AC, de Souza CAF, et al (2025). First reports of *Fusarium agrestense*, *F. gossypinum*, *F. grosmichelii* and *F. triseptatum* causing cassava root rot in Pernambuco, Brazil. Crop Protection 187:106947. https://doi.org/10.1016/j.cropro.2024.106947
6. Dhariwal A, Chong J, Habib S, et al (2017) MicrobiomeAnalyst: a web-based tool for comprehensive statistical, visual and meta-analysis of microbiome data. Nucleic Acids Res 45:W180–W188. https://doi.org/10.1093/nar/gkx295
7. Edwards J, Johnson C, Santos-Medellín C, et al. (2015). Structure, variation, and assembly of the root-associated microbiomes of rice. Proceedings of the National Academy of Sciences 112:.https://doi.org/10.1073/pnas.1414592112
8. Ha J, Gao Y, Zhang R, et al (2021) Diversity of the Bacterial Microbiome Associated With the Endosphere and Rhizosphere of Different Cassava (*Manihot* esculenta Crantz) Genotypes. Front Microbiol 12:.https://doi.org/10.3389/fmicb.2021.729022
9. Howeler RH, Lutaladio N, Thomas G (2013). Save and grow: Cassava. A guide to sustainable production intensification. Food and Agriculture Organisation of the United Nations, Rome. Available at: https://www.fao.org/documents/card/en/c/952504b8-f86d-55e1-8f55-08e6f1f4384d/. Accessed 1 May 2026
10. Huang H, Li M, Guo Q, et al (2024). Influence of Drought Stress on the Rhizosphere Bacterial Community Structure of Cassava (*Manihot* esculenta Crantz). Int J Mol Sci 25:7326. https://doi.org/10.3390/ijms25137326
11. Immanuel S, Jaganathan D, Prakash P, Sivakumar PS (2024) Cassava for food security, poverty reduction and climate resilience: A review. Indian Journal of Ecology 51:21–31. https://doi.org/10.55362/ije/2024/4191
12. Kai M (2020) Diversity and Distribution of Volatile Secondary Metabolites Throughout *Bacillus subtilis* Isolates. Front Microbiol 11:.https://doi.org/10.3389/fmicb.2020.00559
13. Klindworth A, Pruesse E, Schweer T, et al (2013) Evaluation of general 16S ribosomal RNA gene PCR primers for classical and next-generation sequencing-based diversity studies. Nucleic Acids Res 41:e1–e1. https://doi.org/10.1093/nar/gks808
14. Latz E, Eisenhauer N, Rall BC, et al (2012) Plant diversity improves protection against soil-borne pathogens by fostering antagonistic bacterial communities. Journal of Ecology 100:597–604. https://doi.org/10.1111/j.1365-2745.2011.01940.x

15. Liao Q, Shen Z, Li G, et al (2026). Soil microbial community stability: A key to sustainable cassava production. BiolFertil Soils 62:607–628. https://doi.org/10.1007/s00374-026-02000-z
16. Lu J, Breitwieser FP, Thielen P, Salzberg SL (2017) Bracken: estimating species abundance in metagenomics data. PeerJComput Sci 3:e104. https://doi.org/10.7717/peerj-cs.104
17. Lundberg DS, Lebeis SL, Paredes SH, et al (2012) Defining the core Arabidopsis thaliana root microbiome. Nature 488:86–90. https://doi.org/10.1038/nature11237
18. McMurdie PJ, Holmes S (2013) phyloseq: An R Package for Reproducible Interactive Analysis and Graphics of Microbiome Census Data. PLoS One 8:e61217. https://doi.org/10.1371/journal.pone.0061217
19. Mohidin SRNSP, Moshawih S, Hermansyah A, et al (2023). Cassava (*Manihot* esculenta Crantz): A Systematic Review for the Pharmacological Activities, Traditional Uses, Nutritional Values, and Phytochemistry. J Evid Based Integr Med 28:.https://doi.org/10.1177/2515690X231206227
20. Moore E, Arnscheidt A, Kruger A, et al (2008). Section 1 update: Simplified protocols for the preparation of genomic DNA from bacterial cultures. In: Molecular Microbial Ecology Manual. Springer Netherlands, Dordrecht, pp 1905–1919.https://doi.org/10.1007/978-1-4020-2177-0_101
21. Nihorimbere G, Korangi Alleluya V, Nimbeshaho F, et al (2024) *Bacillus*-based biocontrol beyond chemical control in central Africa: the challenge of turning myth into reality. Front Plant Sci 15: https://doi.org/10.3389/fpls.2024.1349357
22. Oksanen J, et al (2026) vegan: Community Ecology Package. R package version 2.7-3. Available at: https://CRAN.R-project.org/package=vegan. Accessed 1 May 2026
23. Oliveira SAS de, Hohenfeld CS, Santos V da S, et al (2013) Resistance to *Fusarium* dry root rot disease in cassava accessions. PesquiAgropecu Bras 48:1414–1417. https://doi.org/10.1590/S0100-204X2013001000014
24. Ongena M, Jacques P (2008) *Bacillus lipopeptides*: versatile weapons for plant disease biocontrol. Trends Microbiol 16:115–125. https://doi.org/10.1016/j.tim.2007.12.009
25. Owino RN, Nguu EK, Obiero GO, Nyaboga EN (2026). Cassava Endophytic Bacteriome as Potential Biocontrol Agents Against Three Crop Phytopathogenic Fungi. Microbiologyopen 15:https://doi.org/10.1002/mbo3.70254
26. Qi W, Song W, Qi R, et al (2025). Land Use Types Drive the Distinct Patterns of Bacterial and Fungal Communities in Soils from the Semi-arid Area. MicrobEcol 88:43. https://doi.org/10.1007/s00248-025-02538-9
27. Raaijmakers JM, Paulitz TC, Steinberg C, et al (2009) The rhizosphere: a playground and battlefield for soilborne pathogens and beneficial microorganisms. Plant Soil 321:341–361. https://doi.org/10.1007/s11104-008-9568-6
28. Saengchan C, Phansak P, Thanh TL, Papathoti NK, Buensanteai N (2021). Efficacy of salicylic acid and a *Bacillus* bioproduct in enhancing growth of cassava and controlling root rot disease. J Plant Prot Res61:260–271.https://doi.org/10.24425/jppr.2021.137952
29. Saengchan C, Sangpueak R, Le Thanh T, et al (2022). Induced resistance against *Fusarium solani* root rot disease in cassava plant (*Manihot* esculenta Crantz) promoted by salicylic acid and *Bacillus subtilis*. Acta Agric Scand B Soil Plant Sci 72:516–526. https://doi.org/10.1080/09064710.2021.2018033
30. Silva IO, Amorim EP da R, Nascimento Junior NA, et al (2022). The first report about *Fusarium falciform*e that causes root rot in cassava cv Rosinha, in Alagoas state, Brazil. Research, Society and Development 11:e221111234369. https://doi.org/10.33448/rsd-v11i12.34369
31. Somyong S, Mhuantong W, Phetchawang P, et al (2025). Influence of organic, synthetic and biofertilizers on the diversity of cassava rhizosphere microbiome in Northeastern Thailand. PeerJ13:e20085. https://doi.org/10.7717/peerj.20085
32. Subhash AP, Veena SS, Makeshkumar T, Anith KN (2025) *Piriformospora indica* and Arbuscular Mycorrhizal Fungus suppress fungal root rot and mosaic diseases of cassava. Symbiosis 95:241–254. https://doi.org/10.1007/s13199-025-01044-3
33. Toju H, Peay KG, Yamamichi M, et al. (2018). Core microbiomes for sustainable agroecosystems. Nat Plants 4:247–257. https://doi.org/10.1038/s41477-018-0139-4
34. Trivedi P, Leach JE, Tringe SG, et al (2020) Plant–microbiome interactions: from community assembly to plant health. Nat Rev Microbiol 18:607–621. https://doi.org/10.1038/s41579-020-0412-1
35. Turner TR, James EK, Poole PS (2013) The plant microbiome. Genome Biol 14:209. https://doi.org/10.1186/gb-2013-14-6-209
36. Tyc, Olaf, Song C, Dickschat JS, et al (2017) The Ecological Role of Volatile and Soluble Secondary Metabolites Produced by Soil Bacteria. Trends Microbiol 25:280–292. https://doi.org/10.1016/j.tim.2016.12.002
37. Ubalua AO, Onyegbula DO, Mbadiwe MN (2020) Pathogenicity and biocontrol potentials of *Bacillus subtilis* on postharvest cassava root rot pathogens. J Emerg Trends EngAppl Sci 11:109–115. https://hdl.handle.net/10520/ejc-sl_jeteas-v11-n3-a2
38. van der Heijden MGA, Hartmann M (2016) Networking in the Plant Microbiome. PLoSBiol14:e1002378. https://doi.org/10.1371/journal.pbio.1002378
39. Vandenkoornhuyse P, Quaiser A, Duhamel M, et al. (2015). The importance of the microbiome of the plant holobiont. New Phytologist 206:1196–1206. https://doi.org/10.1111/nph.13312
40. Vannier N, Agler M, Hacquard S (2019) Microbiota-mediated disease resistance in plants. PLoSPathog15:e1007740. https://doi.org/10.1371/journal.ppat.1007740
41. Versalovic J, de Bruijn FJ, Lupski JR (1998) Repetitive Sequence-based PCR (rep-PCR) DNA Fingerprinting of Bacterial Genomes. In: Bacterial Genomes. Springer US, Boston, MA, pp 437–454.https://doi.org/10.1007/978-1-4615-6369-3_34
42. Vincent JM (1947) Distortion of Fungal Hyphæ in the Presence of Certain Inhibitors. Nature 159:850–850. https://doi.org/10.1038/159850b0

43. Wickham H (2016) Data analysis. In: ggplot2: Elegant graphics for data analysis. Springer International Publishing, Cham, pp 189–201. https://doi.org/10.1007/978-3-319-24277-4
44. Wingett SW, Andrews S (2018) FastQ Screen: A tool for multi-genome mapping and quality control. F1000Res 7:1338. https://doi.org/10.12688/f1000research.15931.2
45. Wood DE, Lu J, Langmead B (2019). Improved metagenomic analysis with Kraken 2. Genome Biol 20:257. https://doi.org/10.1186/s13059-019-1891-0
46. Zaneveld JR, McMinds R, Vega Thurber R (2017). Stress and stability: applying the Anna Karenina principle to animal microbiomes. Nat Microbiol 2:17121. https://doi.org/10.1038/nmicrobiol.2017.121
47. Zapata T, Galindo DM, Corrales-Ducuara AR, Ocampo-Ibáñez ID (2021). The Diversity of Culture-Dependent Gram-Negative Rhizobacteria Associated with *Manihot* esculenta Crantz Plants Subjected to Water-Deficit Stress. Diversity (Basel) 13:366. https://doi.org/10.3390/d13080366
48. Zeng H, Xu H, Liu G, et al (2021) Physiological and metagenomic strategies uncover the rhizosphere bacterial microbiome succession underlying three common environmental stresses in cassava. J Hazard Mater 411:125143. https://doi.org/10.1016/j.jhazmat.2021.125143
49. Zhang L, Zhang J, Wei Y, et al. (2021). Microbiome-wide association studies reveal correlations between the structure and metabolism of the rhizosphere microbiome and disease resistance in cassava. Plant Biotechnol J 19:689–701. https://doi.org/10.1111/pbi.13495

Figures

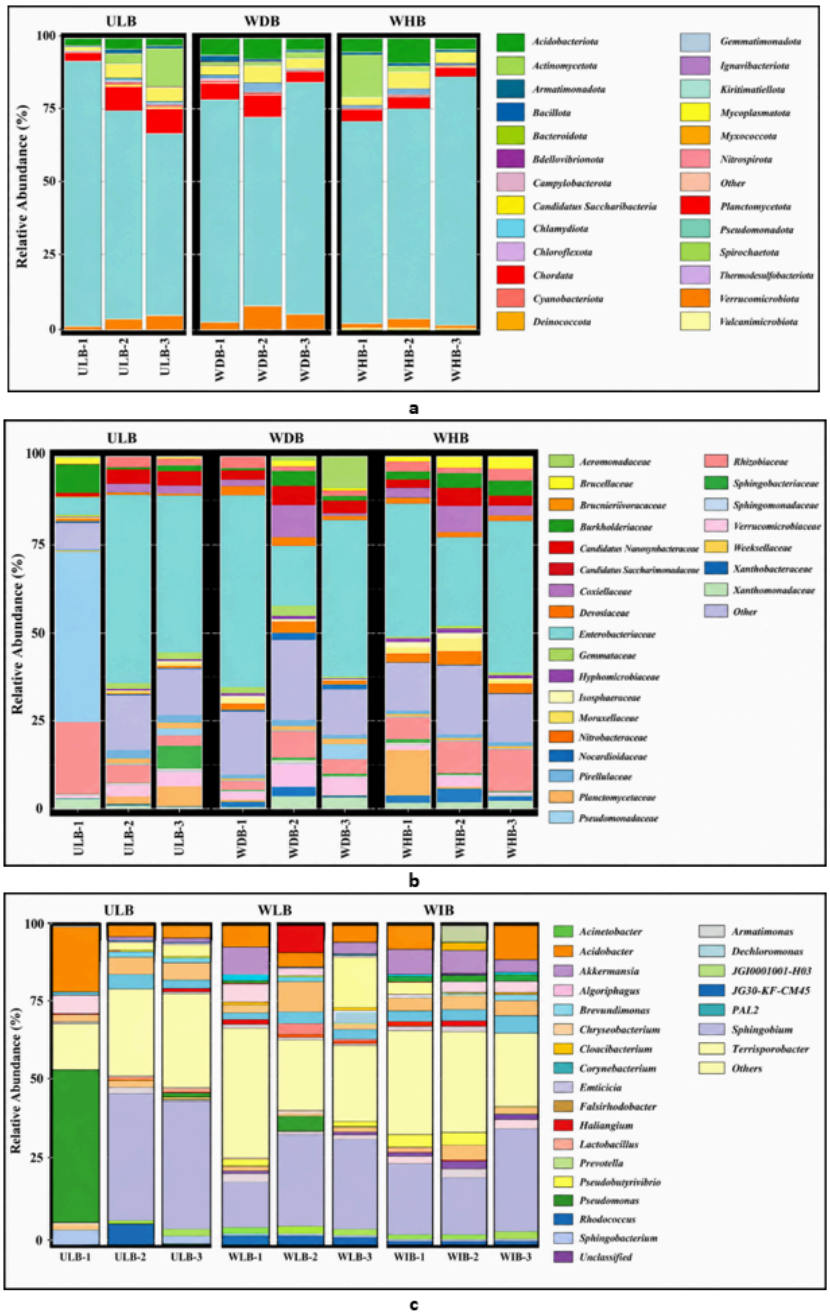

Figure 1

Bacterial community composition of rhizoplane samples, as revealed by 16S rRNA amplicon sequencing: (**a**) phylum-level distribution, (**b**) family-level distribution, and (**c**) genus-level distribution

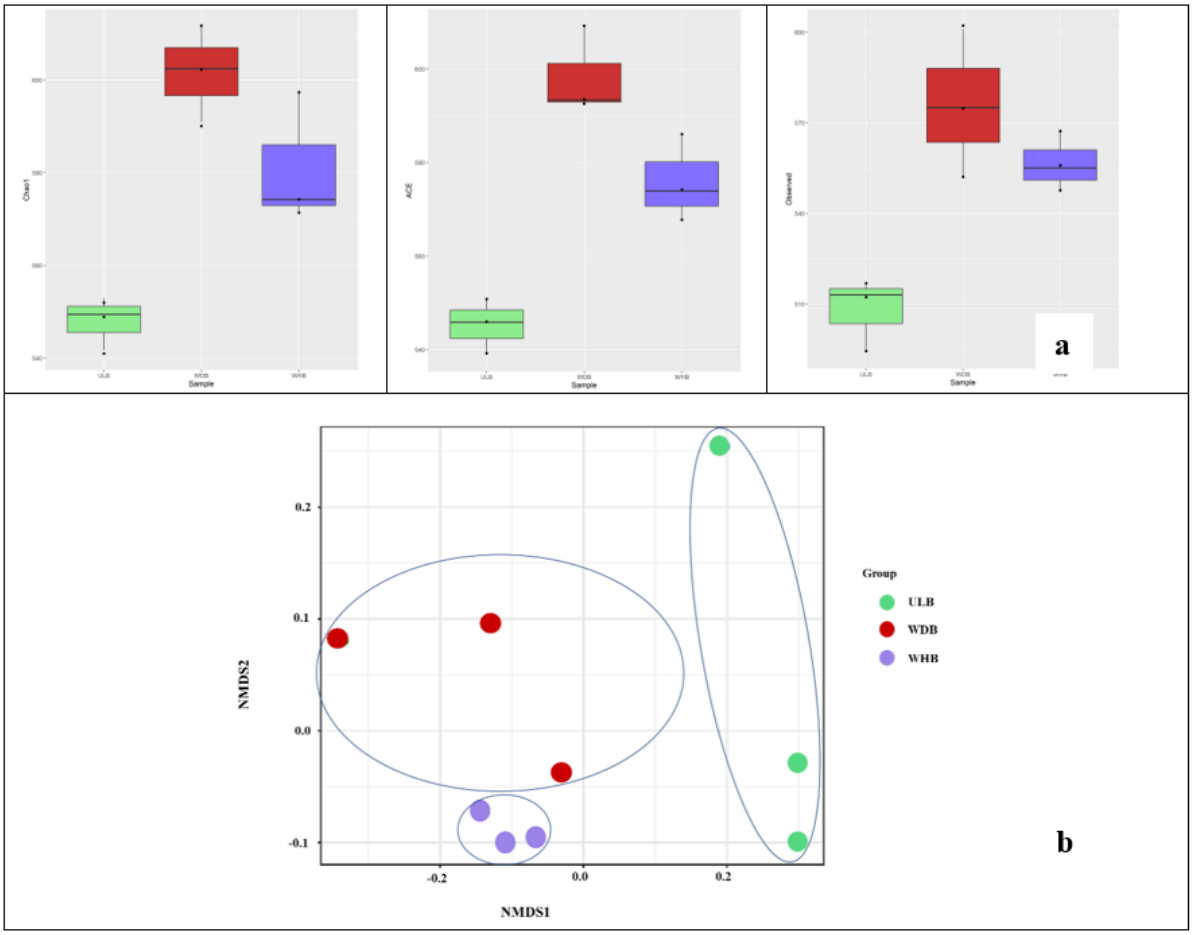

Figure 2

Alpha- and beta-diversity analyses of bacterial communities associated with the cassava rhizoplane. Figure 2**a** presents alpha-diversity indices describing community richness and evenness across agroecosystems, while Figure 2**b** shows a Non-metric Multidimensional Scaling (NMDS) ordination based on Bray–Curtis dissimilarity to evaluate beta-diversity patterns. The NMDS ordination exhibited a low stress value (0.0447), indicating an excellent representation of community relationships in two-dimensional space. PERMANOVA detected no significant differences in overall community composition among groups ($F = 1.229$, $R^2 = 0.29061$, $p = 0.192$)

Note: ULB = upland rhizoplane; WDB = wetland diseased rhizoplane; WHB = wetland healthy rhizoplane

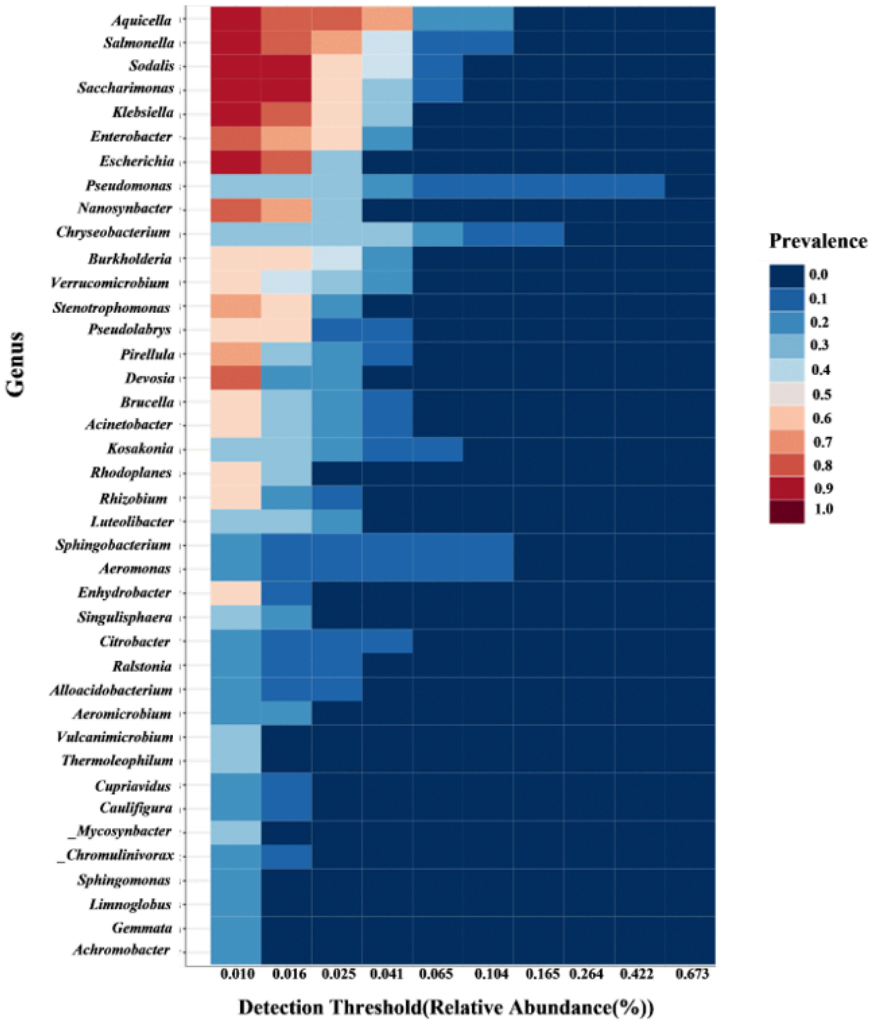

Figure 3

Core bacterial microbiome of the cassava rhizoplane across contrasting agroecosystems

Note: ULB = upland rhizoplane; WDB = wetland diseased rhizoplane; WHB = wetland healthy rhizoplane. The core microbiome comprises bacterial taxa consistently detected across the sampled agroecosystems.

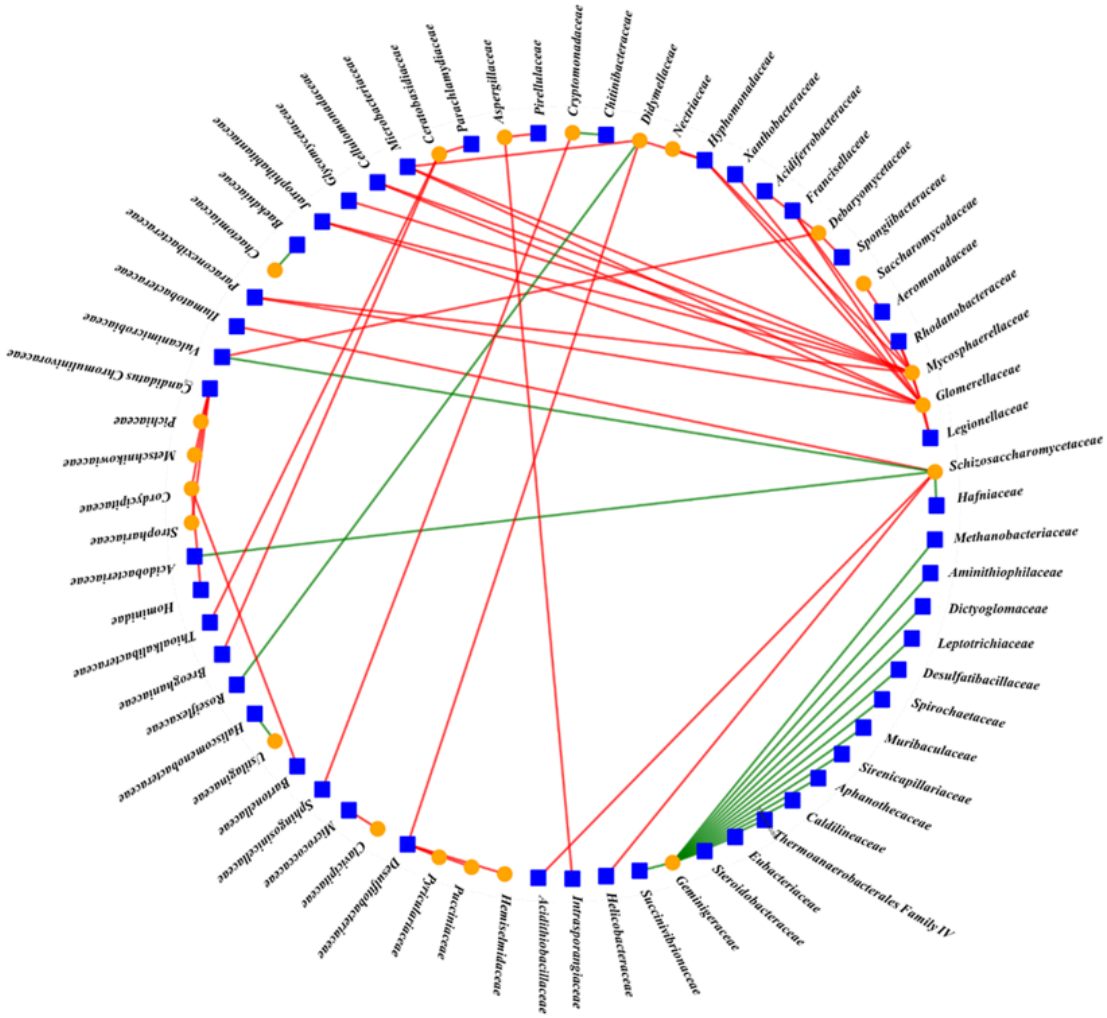

Figure 4

Inter-kingdom co-occurrence network highlighting hub taxa within the cassava rhizoplane microbiome

Nodes represent microbial taxa, with bacterial taxa depicted as blue squares and fungal taxa as orange circles. Edges indicate significant Spearman correlations ($|r| \geq 0.5$, $p < 0.05$; FDR-corrected), where red edges represent positive associations (co-occurrence) and green edges represent negative associations (mutual exclusion).

Treatments	Disease suppressive activity (60 dpi)	Root system of treated plants
Pathogen-inoculated control (T5) × *Bacillus subtilis* ULB_36(T1)		
Pathogen-inoculated control (T5) × *Bacillus sp.*1ULB_12(T2)		
Pathogen-inoculated control (T5) × Chemical control (T3)		
Pathogen-inoculated control (T5) × Untreated control (T4)		

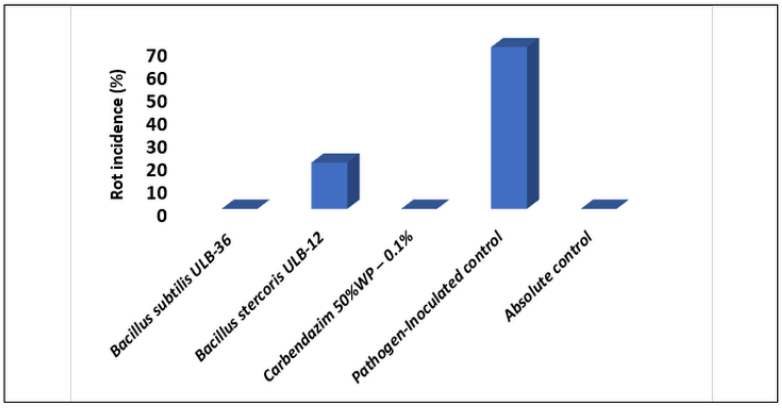

Figure 5

Suppressive effect of cassava rhizoplane bacterial antagonists on stem and root rot under artificial epiphytotic conditions

Supplementary Files

This is a list of supplementary files associated with this preprint. Click to download.

- 4SupplementaryFigures.docx
- 5.SupplementaryTables.docx
- GraohicalAbstract.docx